RSC Advances

PAPER

View Article Online
View Journal | View Issue

Cite this: *RSC Adv.*, 2026, **16**, 4549

Mechanism of action of a boron-dependent antibiotic entails synergistic binding

Shao-Lun Chiou, [a] Jacky Lin,[a] Jiayuan Miao, [b] Yi-Hsuan Tsai,[a] Ching-Wen Chiu, [a] Yu-Shan Lin [b] and John Chu *[ac]

Laspartomycin C (LspC) is a calcium-dependent antibiotic (CDA), a family of peptide antibiotics that has an intriguing mechanism of action (MOA) and great promise in drug development. While it has long been known that CDAs require Ca(II) to function, the mechanistic details remain elusive. We previously reported a synthetic analog of LspC, termed **B1**, that can be fully activated by phenylboronic acid (PBA) and is no longer dependent upon Ca(II) for its antibacterial activity, providing a new entry point to study the MOA of CDAs. In other words, Ca(II) is the cofactor for LspC activation and PBA is the cofactor for **B1** activation. Presented herein is their thorough characterization using isothermal calorimetry, NMR, and molecular dynamics simulation. To our surprise, we found that even though both LspC and **B1** sequester isoprenyl phosphate to suppress bacterial growth, they go through distinct paths. LspC and **B1** have analogous thermodynamic endpoints, namely, a stable ternary complex containing the peptide antibiotic, the cofactor (Ca(II) or PBA), and the substrate. However, the former goes through a binary complex intermediate, whereas for the latter, there is no detectable interaction between any pairs of the three components (**B1**, PBA, and the substrate). **B1** thus presents an extreme case of synergistic binding and a unique way to control the activity of an antibiotic.

Received 5th December 2025
Accepted 14th January 2026

DOI: 10.1039/d5ra09403h

rsc.li/rsc-advances

Introduction

Calcium-dependent antibiotics (CDAs) are peptide antibiotics that require Ca(II) for suppressing bacterial growth.[1] While many enzymes require metal cofactor(s) to operate, this phenomenon is uncommon for natural products, and the mechanistic details remain elusive.[2–5] Members of the CDA family bind to various phospholipid intermediates in the bacterial cell wall biosynthesis pathway, resulting in cell death.[6–8] Such a phospholipid sequestration mechanism is different from most antibiotics currently in clinical use.[9] CDAs are thus promising candidates in addressing the antimicrobial resistance crisis and have attracted the attention of many scientists.[10–13]

Laspartomycin C (LspC) is a cyclic lipopeptide with an N-terminal fatty acyl chain and contains 11 amino acids, including several non-canonical residues such as D-allo-threonine, pipecolic acid, and diaminopropionic acid (Fig. 1a).[10] Previous LspC studies revealed that it has two Ca(II) binding sites and that three aspartate residues (Asp1, Asp5, and Asp7) are critical for its calcium-dependent antibacterial activity.[13,14] LspC is in fact the only CDA that has been structurally characterized in its antibacterially active state (Fig. 1b), which is a ternary complex that includes Ca(II) and geranyl phosphate (C10P). C10P is a surrogate of the important cell wall biosynthesis intermediate undecaprenyl phosphate (C55P).[13,14]

Inspired by this structure, we reported previously a synthetic analogue of LspC, termed **B1**, wherein the functional role of Ca(II) as the cofactor was replaced by phenylboronic acid (PBA) (Fig. 1c).[15] The crystal structure of LspC shows that the side-chain carboxylate of Asp1 and Asp7 coordinate the external Ca(II), and that of the Asp5 coordinates the internal Ca(II). The Asp1 and Asp7 residues in LspC were both substituted with serine in **B1**, whose side-chain hydroxyl groups condense (reversibly) with PBA to form a boronic ester. Calcium cation(s) is hypothesized to hold LspC in a conformation poised for C55P binding, and PBA plays the same role in **B1**. The **B1**/PBA/C10P ternary complex was characterized by mobility shift assays, ^{31}P NMR, and electrospray mass spectrometry.[15]

LspC and **B1** both bind the same isoprenyl phosphate substrate and form analogous ternary complexes, *i.e.*, LspC/Ca(II)/C10P and **B1**/PBA/C10P. In LspC, the electrostatic attraction between the external Ca(II) and the phosphate of C55P is key to sequestering C55P. Similarly, the empty boron p orbital in PBA after it condenses with **B1** engages the phosphate oxyanion. Herein, we report isothermal calorimetry (ITC), nuclear magnetic resonance (NMR), and molecular dynamics (MD) simulation data to show that these two peptide antibiotics

[a]*Department of Chemistry, National Taiwan University, No. 1 Section 4, Roosevelt Road, Taipei City 10617, Taiwan. E-mail: johnchu@ntu.edu.tw*

[b]*Department of Chemistry, Tufts University, 62 Talbot Avenue, Medford, MA 02155, USA*

[c]*Center for Emerging Material and Advanced Devices, National Taiwan University, No. 1 Section 4, Roosevelt Road, Taipei City 10617, Taiwan*

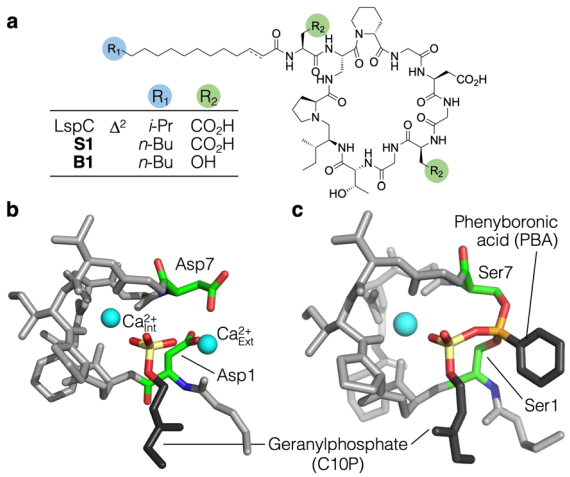

Fig. 1 (a) In the current study, **S1** served as the surrogate of LspC. They are identical except for a minor difference in the N-terminal fatty acyl chain (R_1 and unsaturation (Δ^2)). The two aspartic acid residues (Asp1 and Asp7) that interacts with the external Ca(II), marked in green, are replaced with serine in the synthetic analogue **B1**. (b) LspC was co-crystallized with Ca(II) and C10P in its active conformation (PDB ID: 5O0Z).[14] (c) MD simulation shows that the **B1**/PBA/C10P/Ca(II) quaternary complex adopts a structure highly similar to that of **S1**/Ca(II)/C10P.

arrive at analogous thermodynamic endpoints *via* distinct paths. The former undergoes stepwise binding and an intermediate binary complex, whereas the latter is a rare example among small molecules of synergistic binding. Specifically, while the formation of the **B1**/PBA/C10P ternary complex is highly favourable, mixing any two of the three components (**B1**, PBA, and C10P) showed no detectable interaction. Such a unique phenomenon suggests that the conformational change of **B1** is not stepwise and only occurs in the presence of both PBA and C10P, offering new possibilities in small molecule drug design and engineering.

Results

Characterization of C10P binding by ITC

We started by using ITC to assess the substrate affinity of these peptide antibiotics. In this study, **S1** was used as a surrogate of LspC (Fig. 1a). These two peptide antibiotics are identical except for a minor difference in their N-terminal fatty acyl chains and show no detectable differences in antibacterial potencies and MOA.[15] Our first set of experiments was performed in 20 mM HEPES buffer (pH 7.4) supplemented with 5 mM of $CaCl_2$. Titrating C10P into the sample cell containing a solution of **B1** (50 μM) premixed with 250 μM of PBA resulted in an exothermic binding isotherm with a near equimolar stoichiometry [$K_d = (2.0 \pm 1.1) \times 10^{-7}$ M, $n = 1.14 \pm 0.05$, Fig. 2a]. Titrating C10P into **S1** (500 μM) also resulted in an exothermic binding isotherm, albeit with slightly weaker binding [$K_d = (2.5 \pm 1.9) \times 10^{-6}$ M, $n = 0.79 \pm 0.10$, Fig. 2b]. All ITC experiments were repeated in triplicate (Fig. S1 to S8). These results suggest that in the presence of the appropriate cofactor, *i.e.*, Ca(II) for **S1** and PBA for **B1**, both peptide antibiotics form an equimolar complex with the phospholipid substrate C10P.

Next, we investigated the importance of Ca(II) for **S1** and **B1**. The buffers used in these experiments remained the same,

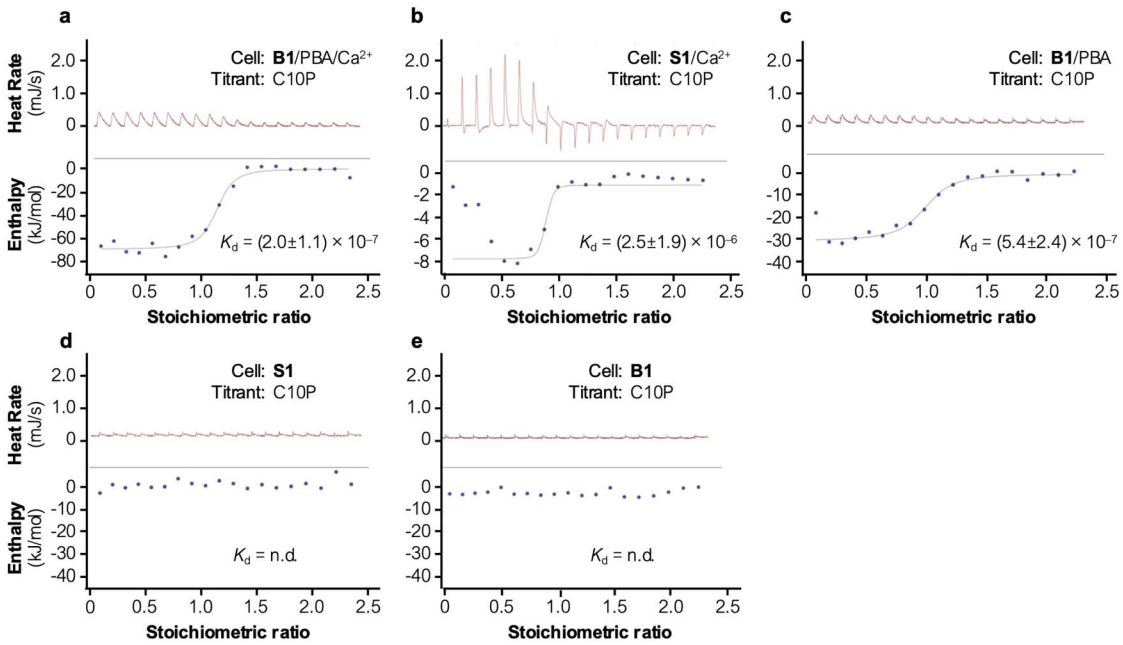

Fig. 2 Representative traces of C10P titration into (a) **B1**/PBA/Ca^{2+} and (b) **S1**/Ca^{2+} in the presence of 5 mM Ca(II). Note that the first three outlier datapoints in (b) were excluded from analysis. Such a pattern is due to **S1** aggregation and was also observed in ITC studies of LspC in previous reports.[13] Representative traces of C10P titration into (c) **B1**/PBA, (d) **S1**, and (e) **B1** with no supplemented Ca(II). All ITC experiments were performed in triplicate ($n = 3$) in the same buffer solution (150 mM NaCl, 20 mM HEPES, at pH 7.4). The rest of the ITC traces can be found in the Supporting Information (SI) (Fig. S1 to S8).

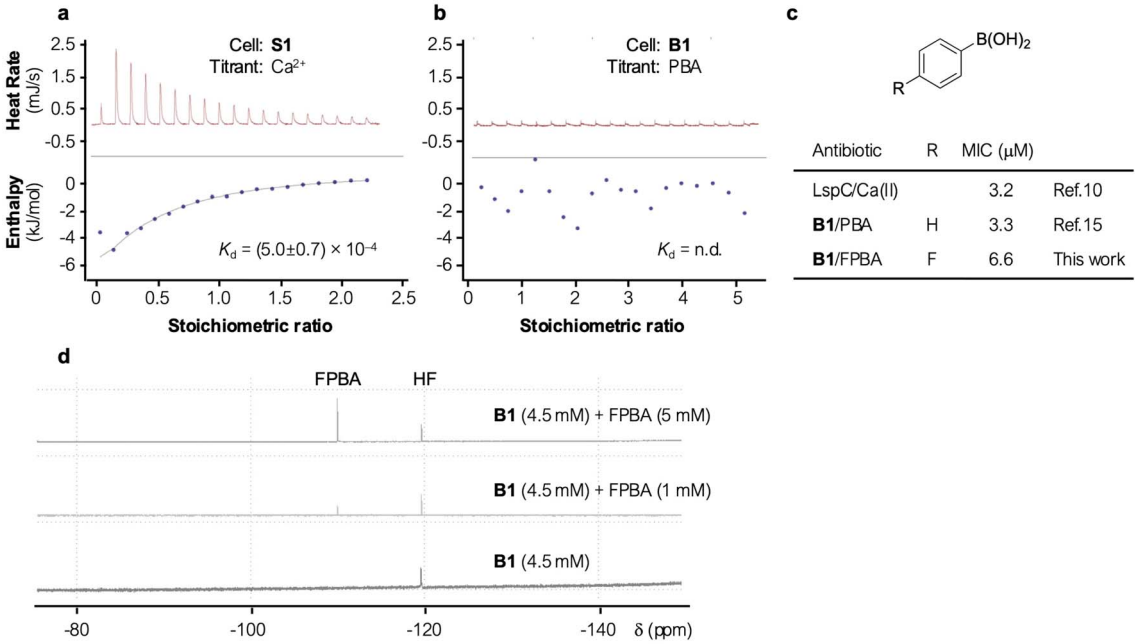

Fig. 3 Representative traces of (a) Ca^{2+} titration into **S1** and (b) PBA titration into **B1**. All ITC experiments were performed in triplicate in the same buffer solution (150 mM NaCl, 20 mM HEPES, at pH 7.4). The rest of the ITC traces can be found in the SI (Fig. S1 to S8). (c) Minimal inhibitory concentrations (MIC) of various peptide antibiotics against *Staphylococcus aureus* ATCC 29213. (d) ^{19}F NMR spectra of **B1** were acquired in the same HEPES buffer described in the main text in the presence of 0, 1, and 5 mM of FPBA; hydrogen fluoride (HF) was included as the internal standard.

Table 1 ITC characterization of **S1** and **B1**

Analyte	Titrant	K_d (M)
S1	Ca(II)	$(5.0 \pm 0.7) \times 10^{-4}$
S1	C10P	No interaction
S1/Ca(II)	C10P	$(2.5 \pm 1.9) \times 10^{-6}$
B1	Ca(II)	No interaction
B1	C10P	No interaction
B1/PBA	C10P	$(2.0 \pm 1.1) \times 10^{-7}$
B1	PBA	No interaction (est. > 0.2) [a]
PBA	C10P	No interaction

[a] Estimated based on ^{19}F NMR characterization of a **B1**/FPBA mixture. See SI for details.

except for the lack of Ca(II) supplement. The apparent C10P affinity for the **B1**/PBA mixture was similar [$K_d = (5.4 \pm 2.4) \times 10^{-7}$ M, Fig. 2c], whereas no binding was observed for **S1** (Fig. 2d). These observations are in line with the fact that CDAs, such as **S1**, depend on Ca(II) to function.[10] In contrast, **B1** showed no Ca(II) dependence but completely lost its affinity for C10P in the absence PBA (Fig. 2e). These results support the notion that **S1** is a calcium-dependent antibiotic and **B1** is a boron-dependent antibiotic.[15]

S1 and Ca(II) form a binary complex; B1 and PBA do not

In our design, PBA in **B1** was meant to replace the role of Ca(II) in **S1** as a cofactor, inducing the peptide backbone to adopt a conformation that is poised to bind the isoprenyl phosphate substrates (C10P or C55P). We were therefore interested in the thermodynamic landscape that leads up to C10P binding. Titrating $CaCl_2$ into **S1** (500 μM) showed a binding isotherm with moderate affinity that is consistent with previous reports [$K_d = (5.0 \pm 0.7) \times 10^{-4}$ M (stoichiometry fixed at $n = 2$ for curve fitting, Fig. 3a].[16] In contrast, we did not find evidence of **B1**/PBA binary complex formation as no ITC signal was observed when PBA was titrated into **B1** (Fig. 3b).

One possibility for no apparent **B1**/PBA binding in ITC is that this condensation reaction is strongly favourable but proceeds too slowly. As an extreme example, condensation between PBA and *cis*-1,2-cyclopantanediol has forward and reverse rate constants of $k_{on} = 0.022\ M^{-1}s^{-1}$ and $k_{off} = 0.0014\ s^{-1}$, respectively (Table S1). It is estimated that a boronic acid and a diol with these rate constants under our experimental conditions would take ~50 minutes to reach equilibrium (see SI).[17,18] We therefore extended the intervals between injections to one hour and still saw no ITC signals. Another possibility is that the **B1**/PBA interaction is in fact too weak to be detected by ITC, and we decided to use ^{19}F NMR spectroscopy to assess the **B1**/PBA interaction (if any).

Fluorine (^{19}F) NMR is useful for its high sensitivity. In addition, since biomolecules rarely contain fluorine, ^{19}F NMR spectra interpretation is straightforward.[19] We first confirmed that 4-fluorophenylboronic acid (FPBA) was able to activate **B1** and the resulting antibacterial activity is comparable to that of **B1**/PBA (Fig. 3c). PBA and FPBA suppressed *Staphylococcus aureus* growth with a minimum inhibitory concentration (MIC) of 3.3 and 6.6 μM, respectively.[15] Our ^{19}F NMR experiments were performed in the same HEPES buffer (pH 7.4) with 10% (v/v)

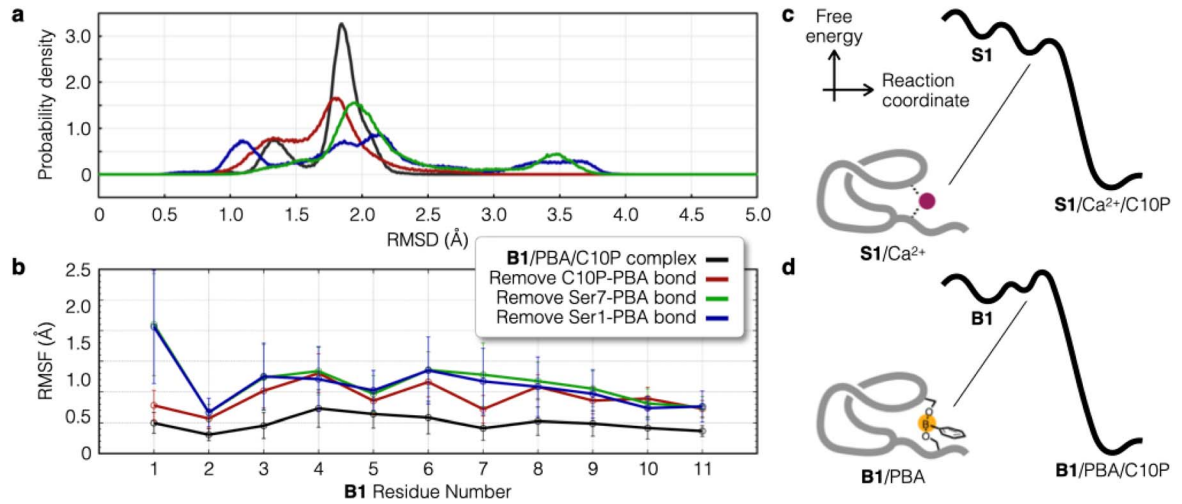

Fig. 4 The **B1**/PBA/C10P ternary complex has three B–O bonds. They were removed one at a time to generate three new complexes. Shown herein are the (a) RMSD and (b) RMSF of MD simulations performed on these structures. Each trace represents the average of five parallel simulations (Fig. S11 and S12). Free energy landscape of (c) **S1**/Ca(II)/C10P and (d) **B1**/PBA/C10P formation. Data presented herein suggest that en route to their respective ternary complex, **S1**/Ca(II) forms a binary complex whereas **B1**/PBA does not.

D_2O in the presence of hydrogen fluoride (HF) as the internal standard (δ −119.7 ppm). First, we showed that FPBA condenses with a vicinal diol (glucose) and results in an unmistakable upfield shift in ^{19}F signal (δ from −110 to −118 ppm, Fig. S9). A series of ^{19}F NMR spectra of **B1** supplemented with 0, 1, and 5 mM of FPBA was then acquired. The mixtures were incubated at room temperature for at least one hour to ensure that boronic ester formation (if any) has reached equilibrium. No new ^{19}F signal was observed (Fig. 3d). Based on the experimental conditions and the detection limit of our ^{19}F NMR spectrometer, these results suggest that the **B1**/PBA interaction (if any) is extremely weak (K_d estimated to be greater than 0.2 M, see SI for details).

No pairwise interactions between B1, PBA, and C10P

Aside from no detectable interaction between **B1**/PBA, we also did not detect any **B1**/C10P (Fig. 1e) or PBA/C10P interaction (Fig. S10). In other words, there is no appreciable pairwise interaction among any of these three molecular entities (**B1**, PBA, and C10P). This system thus presents a rare example of strong synergistic binding, wherein a highly stable complex forms only when all three components are present without going through a binary intermediate complex (Table 1). The mechanism of **S1** is different as its formation of the **S1**/Ca(II)/C10P ternary complex is stepwise. ITC data showed that **S1** and Ca(II) engage in weak yet clearly detectable binding [K_d = $(4.4 \pm 0.4) \times 10^{-4}$ M].

Insights from MD simulations

We then looked to molecular dynamics (MD) simulation to gain insight into **B1**/PBA/C10P synergistic binding. Each of the three oxygen–boron (B–O) bonds in the **B1**/PBA/C10P ternary complex (C10P (phosphate)-PBA, Ser7-PBA, and Ser1-PBA) was removed to generate three separate complexes as the starting point for MD simulation. In these structures, the boron atoms were sp^2 hybridized with an empty p orbital and adopt a trigonal planar geometry (Fig. S11). The simulations showed that removing any of the three oxygen-boron bonds (C10P-PBA, Ser7-PBA, or Ser1-PBA) resulted in a more flexible structure that began to gradually deviate from the antibacterially active conformation (Fig. S11 and S12). The extent of movement was quantitated by measuring the root-mean-square deviation (RMSD, Fig. 4a) relative to the initial structure and root-mean-square fluctuation over time (RMSF, Fig. 4b). For residues other than Ser1 and Ser7, these three structures displayed similar RMSF and RMSD probability density distributions. The averaged RMSDs for the complex missing the C10P–PBA, Ser7–PBA, and Ser1–PBA bonds are within standard errors (1.69 ± 0.15, 2.22 ± 0.52, and 2.08 ± 0.81 Å, respectively). These results suggest that the three B–O bonds contributed nearly equally to stabilizing the **B1**/PBA/C10P ternary complex, as would be expected for a three-component synergistic binding system. If **B1**/PBA was a stable intermediate *en route* the eventual **B1**/PBA/C10P ternary complex, MD simulation of the latter two (removing the Ser7–PBA or Ser1–PBA bonds) would have destabilized the complex to a much greater extent and manifest as greater movements due to the removal of B–O bonds. Together, the ITC, NMR, and MD simulation results are consistent with synergistic binding, wherein the combined effect is much greater than the sum of their separate effects.

Conclusion and discussion

We report herein the mechanistic study of a boron-dependent antibiotic (BDA) **B1**, a synthetic analog of the CDA **S1**, using ITC, NMR, and MD simulation. These two peptide antibiotics inhibit bacterial growth by forming analogous ternary complexes to sequester the key cell wall biosynthesis intermediate C55P (**B1**/PBA/C10P and **S1**/Ca(II)/C10P). While they show comparable affinities for C10P, a surrogate of C55P soluble in

aqueous solutions, their paths *en route* the final ternary complex are different despite having the same target substrate and analogous thermodynamic endpoints. Specifically, our data suggest that **S1** forms an intermediate binary complex with Ca(II) and then bind C10P (Fig. 4c), whereas **B1** shows synergistic binding with no discernable intermediate (Fig. 4d).

Synergistic binding describes the phenomenon wherein presenting two (or more) molecular entities simultaneously shows a far greater affinity for the host than their individual affinities combined. This phenomenon is reminiscent of the *Luban Lock*, a traditional Chinese wooden toy that requires the assembly of all pieces in the correct arrangement to form a locked structure. The **B1**/PBA/C10P ternary complex reported herein is unique in two ways even among synergistic binding systems. First, while cases of protein-ligand synergistic interactions have been reported, small molecule systems are extremely rare.[20–24] The binding and release of molecular oxygen by hemoglobin is a classic example, wherein early binding events induce conformational changes that make subsequent binding events more favorable.[25,26] Second, the early binding events that lead up to the eventual synergistic complex are usually weak but still detectable. An example is the DNA synthesis complex, wherein the three molecular species involved are the enzyme (E), *i.e.*, DNA polymerase and the primer/template complex, the metal cofactor (Mg(II)), and the substrate (dNTP). The magnesium cation has only weak interaction with dNTP (K_d ~0.1 mM), and the other pairs (E/Mg(II) and E/dNTP) do not have detectable interactions.[27,28]

Note that neither of the above are perfect examples. Our **B1**/PBA/C10P complex is an extreme case that has no discernable intermediate, and to the best of our knowledge, synergistic binding systems with these features are unprecedented among small molecules.[29–32] In the context of the peptide antibiotic **B1**, synergistic binding can be viewed as a manifestation of specificity and a way to control activity, as it shows no affinity for the isoprenyl phosphate substrate (C10P) in the absence of PBA, and *vice versa*. Such a control mechanism would be useful in the development of targeted anticancer drugs, for example, wherein a molecular toxin is designed to be turned on only in the presence of a tumor-specific molecule. Whether such a phenomenon is general to other CDA synthetic analogs remains to be seen. We are also exploring the possibility of applying such a design principle to other bioactive small molecules.

Author contributions

Peptide synthesis and characterizations were performed by SLC. ITC measurements were performed by SLC and JL. Fluorine NMR was performed by SLC, YHT, and CWC. Molecular dynamics simulations were performed by JM and YSL. SLC and JC conceptualized this project and wrote the manuscript.

Conflicts of interest

There are no conflicts to declare.

Data availability

The data that support the findings of this study are available in the supplementary information (SI). Supplementary information: methods, analytical data, ITC traces, MD simulation preparation and analysis, supplementary figures and tables. See DOI: https://doi.org/10.1039/d5ra09403h.

Acknowledgements

This work was supported by grants from National Science and Technology Council of Taiwan (NSTC 113-2628-M-002-014-MY4), National Taiwan University (NTU-114L8527 and NTU-CC-113L895203), and the National Institute of General Medical Sciences of the National Institutes of Health (R01GM124160, principal investigator: Y.-S. Lin).

References

1 T. M. Wood and N. I. Martin, *MedChemComm*, 2019, **10**, 634–646.
2 S.-L. Chiou, C.-Y. Chang and J. Chu, *ChemMedChem*, 2025, e202400498.
3 D. Jung, A. Rozek, M. Okon and R. E. Hancock, *Chem. Biol.*, 2004, **11**, 949–957.
4 G. Bunkóczi, L. Vértesy and G. M. Sheldrick, *Acta Crystallogr. D Struct. Biol.*, 2005, **61**, 1160–1164.
5 F. Grein, A. Müller, K. M. Scherer, X. Liu, K. C. Ludwig, A. Klöckner, M. Strach, H.-G. Sahl, U. Kubitscheck and T. Schneider, *Nat. Commun.*, 2020, **11**, 1455.
6 S. D. Taylor and M. Palmer, *Bioorg. Med. Chem.*, 2016, **24**, 6253–6268.
7 B. M. Hover, S. H. Kim, M. Katz, Z. Charlop-Powers, J. G. Owen, M. A. Ternei, J. Maniko, A. B. Estrela, H. Molina, S. Park, D. S. Perlin and S. F. Brady, *Nat. Microbiol.*, 2018, **3**, 415–422.
8 C. Wu, Z. Shang, C. Lemetre, M. A. Ternei and S. F. Brady, *J. Am. Chem. Soc.*, 2019, **141**, 3910–3919.
9 W. R. Miller and C. A. Arias, *Nat. Rev. Microbiol.*, 2024, **22**, 598–616.
10 L. H. J. Kleijn, S. F. Oppedijk, P. T. Hart, R. M. Van Harten, L. A. Martin-Visscher, J. Kemmink, E. Breukink and N. I. Martin, *J. Med. Chem.*, 2016, **59**, 3569–3574.
11 M. Heidary, A. D. Khosravi, S. Khoshnood, M. J. Nasiri, S. Soleimani and M. Goudarzi, *J. Antimicrob. Chemother.*, 2017, **73**, 1–11.
12 S. W. Ho, D. Jung, J. R. Calhoun, J. D. Lear, M. Okon, W. R. P. Scott, R. E. W. Hancock and S. K. Straus, *Eur. Biophys. J.*, 2008, **37**, 421–433.
13 T. M. Wood, M. R. Zeronian, N. Buijs, K. Bertheussen, H. K. Abedian, A. V. Johnson, N. M. Pearce, M. Lutz, J. Kemmink, T. Seirsma, L. W. Hamoen, B. J. C. Janssen and N. I. Martin, *Chem. Sci.*, 2022, **13**, 2985–2991.
14 L. H. J. Kleijn, H. C. Vlieg, T. M. Wood, J. Sastre Toraño, B. J. C. Janssen and N. I. Martin, *Angew. Chem., Int. Ed.*, 2017, **56**, 16546–16549.

15 S.-L. Chiou, Y.-J. Chen, C.-T. Lee, M. N. Ho, J. Miao, P.-C. Kuo, C.-C. Hsu, Y.-S. Lin and J. Chu, *Angew. Chem., Int. Ed.*, 2024, **63**, e202317522.
16 I. Kotsogianni, T. M. Wood, F. M. Alexander, S. A. Cochrane and N. I. Martin, *ACS Infect. Dis.*, 2021, **7**, 2612–2619.
17 E. Watanabe, C. Miyamoto, A. Tanaka, K. Iizuka, S. Iwatsuki, M. Inamo, H. D. Takagi and K. Ishihara, *Dalton Trans.*, 2013, **42**, 8446–8453.
18 B. Kang and J. A. Kalow, *ACS Macro Lett.*, 2022, **11**, 394–401.
19 D. Gimenez, A. Phelan, C. D. Murphy and S. L. Cobb, *Beilstein J. Org. Chem.*, 2021, **17**, 293–318.
20 A. Ghode, L. Z. F. Gross, W.-V. Tee, E. Guarnera, I. N. Berezovsky, R. M. Biondi and G. S. Anand, *Biophys. J.*, 2020, **119**, 1833–1848.
21 S. K. Ramisetty and R. S. Dias, *J. Mol. Liq.*, 2015, **210**, 64–73.
22 E. O. Mazzoni, S. Mahony, M. Closser, C. A. Morrison, S. Nedelec, D. J. Williams, D. An, D. K. Gifford and H. Wichterle, *Nat. Neurosci.*, 2013, **16**, 1219–1227.
23 F. Du, F. Navarro-Garcia, Z. Xia, T. Tasaki and A. Varshavsky, *Proc. Natl. Acad. Sci. U. S. A.*, 2002, **99**, 14110–14115.
24 T. S. Beyett, C. To, D. E. Heppner, J. K. Rana, A. M. Schmoker, J. Jang, D. J. H. De Clercq, G. Gomez, D. A. Scott, N. S. Gray, P. A. Jänne and M. J. Eck, *Nat. Commun.*, 2022, **13**, 2530.
25 W. A. Eaton, E. R. Henry, J. Hofrichter and A. Mozzarelli, *Nat. Struct. Biol.*, 1999, **6**, 351–358.
26 M. Bringas, A. A. Petruk, D. A. Estrin, L. Capece and M. A. Martí, *Sci. Rep.*, 2017, **7**, 10926.
27 J. E. Wilson and A. Chin, *Anal. Biochem.*, 1991, **193**, 16–19.
28 K. A. Johnson, *Biochim. Biophys. Acta*, 2010, **1804**, 1041–1048.
29 M. Bastos, O. Abian, C. M. Johnson, F. Ferreira-da-Silva, S. Vega, A. Jimenez-Alesanco, D. Ortega-Alarcon and A. Velazquez-Campoy, *Nat. Rev. Methods Primers*, 2023, **3**, 17.
30 X. Du, Y. Li, Y. L. Xia, S. M. Ai, J. Liang, P. Sang, X. L. Ji and S. Q. Liu, *Int. J. Mol. Sci.*, 2016, **17**, 144.
31 H. Su and Y. Xu, *Front. Pharmacol*, 2018, **9**, 1133.
32 J. F. Gaucher, M. Reille-Seroussi and S. Broussy, *Chemistry*, 2022, **28**, e202200465.